Charge-Transfer Salts of Octamethylferrocenyl Thioethers with Organic Acceptors (TCNQ and $TCNQF_4$) and Trihalides (Br_3^- and I_3^-). Synthesis, Structure, and Physical Properties

Stefan Zürcher, Jeannine Petrig, Volker Gramlich,† Michael Wörle,† Christian Mensing,‡ Dieter von Arx,§ and Antonio Togni*

Laboratory of Inorganic Chemistry, ETH Zentrum, Swiss Federal Institute of Technology, CH-8092 Zürich, Switzerland

Received March 24, 1999

Six charge-transfer (CT) complexes containing three different octamethylferrocene derivatives ($Fe(\eta^5\text{-}C_5Me_4SMe)_2$, **1**; $Fe(\eta^5\text{-}C_5Me_4S^tBu)_2$, **2**; $Fe(\eta^5\text{-}C_5Me_4S)_2S$, **3**) and TCNQ or $TCNQF_4$, respectively (**4**−**9**), have been prepared and fully characterized. X-ray crystal structural studies of **4**, **5**, **7**, and **9** have been carried out. The CT complexes **4** and **5**, containing TCNQ, display stacks of acceptor molecules with noncommon donor/acceptor stoichiometries of 3:7 for **4** and 1:3 for **5**, whereas the charge-transfer complexes **7** and **9**, containing $TCNQF_4$, display strongly interacting dimers of acceptor anions. The compounds **4**−**6** behave as semiconductors with room-temperature conductivities up to 3.5 S cm^{-1} for **6**. Magnetic susceptibility measurements indicate strong antiferromagnetic interaction for the $(TCNQF_4)_2^{2-}$ dimers in **7**−**9**, the dimers being diamagnetic ($S = 0$) at room temperature. Antiferromagnetic interactions are also observed for the three compounds **4**−**6**. To obtain more accurate *Landé-g* factors for the three possible cations from **1**−**3**, the corresponding trihalogenide salts with Br_3^- (**10**−**12**) and I_3^- (**13**−**15**) were prepared and fully characterized. Their magnetic properties, only deriving from the cations, were measured, and X-ray crystal structural studies have been carried out for the compounds **11**, **12**, **14**, and **15**. For the two compounds containing the *tert*-butyl substituent (**11** and **14**), a DADA structural motif was observed, and with the trithiaferrocenophanium, chains (**12**) and networks (**15**) of alternating sulfur bridges and trihalogenide anions were observed.

Introduction

In continuation of our studies concerning CT complexes with ferrocene donor molecules,[1−5] in particular the recently described 1,1′-bis(alkylthio)octamethylferrocenes,[1] we report herein the synthesis and structural and physical characterization of CT complexes corresponding to the six combinations of donors **1**−**3** and the acceptors TCNQ and $TCNQF_4$, respectively (see Scheme 1). In general, depending on the redox potential and the steric demand of the donor molecules, TCNQ-containing complexes show different stoichiometries (donor-to-acceptor ratio), such as 1:1,[6] 1:2,[2,7−9] 1:3,[10,11] 1:4,[12,13] and 2:5,[14] although other proportions have been observed. Several organometallic derivatives containing TCNQ or $TCNQF_4$ have also been reported.[2,15−44] These materials turn out to be either insulators (e.g., the 1:1

† X-ray crystallographic studies.
‡ Conductivity measurements.
§ Magnetic susceptibility measurements.

(1) Zürcher, S.; Gramlich, V.; von Arx, D.; Togni, A. *Inorg. Chem.* **1998**, *37*, 4015−4021.
(2) Hobi, M.; Rihs, G.; Rist, G.; Albinati, A.; Zanello, P.; Zech, D.; Keller, H.; Togni, A. *Organometallics* **1994**, *13*, 1224−1234.
(3) Hobi, M.; Zürcher, S.; Gramlich, V.; Burckhardt, U.; Mensing, C.; Spahr, M.; Togni, A. *Organometallics* **1996**, *15*, 5342−5346.
(4) Hobi, M. J. Ferrocene als Donoren in Charge-Transfer-Komplexen. Ph.D. Thesis No. 12184, Eidgenössische Technische Hochschule (ETH), Zürich, 1997.
(5) Hobi, M.; Ruppert, O.; Gramlich, V.; Togni, A. *Organometallics* **1997**, *16*, 1384−1391.
(6) Kusakawa, H.; Akashi, K. *Bull. Chem. Soc. Jpn.* **1969**, *42*, 263−265.
(7) Moore, A.; Skabara, P. J.; Bryce, M. R.; Batsanov, A. S.; Howard, J. A. K.; Daley, S. T. K. *J. Chem. Soc., Chem. Commun.* **1993**, 417−419.
(8) Swietlik, R.; Graja, A.; Sopa, E.; Zelezny, V.; Petzelt, J. *J. Mol. Struct.* **1984**, *115*, 165−168.
(9) Shibaeva, R. P.; Kaminskii, V. F.; Simonov, M. A. *Cryst. Struct. Commun.* **1980**, *9*, 655−661.
(10) Wang, H.; Chen, Y.; Li, J. *Inorg. Chim. Acta* **1988**, *148*, 261−264.
(11) Nakashima, S.; Sano, H. *Bull. Chem. Soc. Jpn.* **1989**, *62*, 3012−3014.
(12) Lequan, R. M.; Lequan, M.; Legeay, P. *J. Organomet. Chem.* **1987**, *323*, 77−81.
(13) Ward, M. D.; Calabrese, J. C.; Johnson, D. C.; Fagan, P. J. *J. Am. Chem. Soc.* **1989**, *111*, 1719−1732.
(14) Kobayashi, H.; Danno, T.; Saito, Y. *Acta Crystallogr.* **1973**, *B29*, 2693−2699.
(15) Shibaeva, R. P.; Shvets, A. E.; Atovmyan, L. O. *Dokl. Akad. Nauk SSSR* **1971**, *199*, 334−339.
(16) Shibaeva, R. P.; Atovmyan, L. O.; Rozenberg, L. P. *Zh. Strukt. Khim.* **1975**, *16*, 147−150.
(17) Shibaeva, R. P.; Atovmyan, L. O.; Ponomarev, V. I. *Zh. Strukt. Khim.* **1975**, *16*, 860−884.
(18) Lau, C.; Singh, P.; Cline, S.; Seiders, R.; Brookhart, M.; Marsh, W. E.; Hodgson, D. J.; Hatfield, W. E. *Inorg. Chem.* **1982**, *21*, 208−212.
(19) Gallucci, J. C.; Opromolla, G.; Paquette, L. A.; Pardi, L.; Schirch, F. T.; Sivik, M. R.; Zanello, P. *Inorg. Chem.* **1993**, *32*, 2292−2297.
(20) Zhang, J. H.; Reiff, W. M.; Miller, J. S. *Inorg. Chem.* **1987**, *26*, 600−608.
(21) Lequan, R. M.; Lequan, M.; Jaouen, G.; Ouahab, L.; Batail, P.; Padiou, J.; Sutherland, G. *J. Chem. Soc., Chem. Commun.* **1985**, 116−118.

10.1021/om9902075 CCC: $18.00
Publication on Web 08/05/1999

Scheme 1

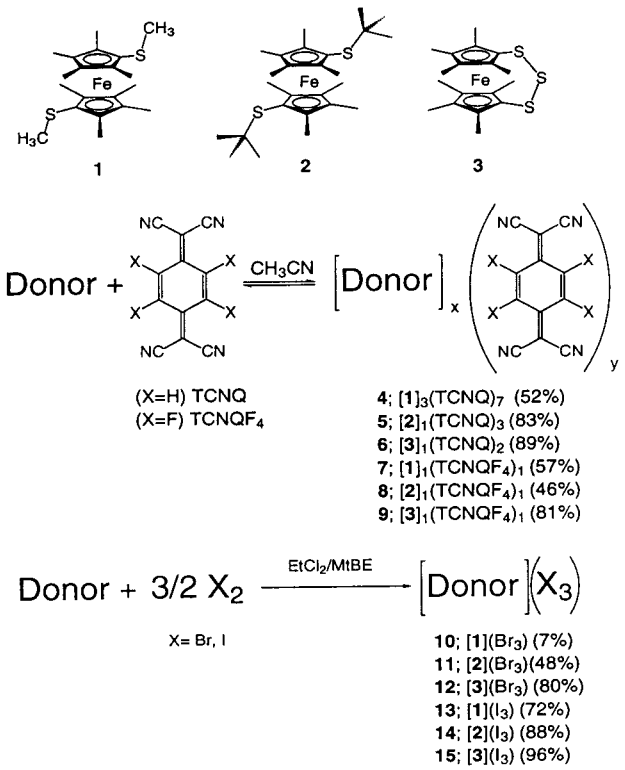

salts containing ammonium cations) or semiconductors (e.g., the mixed valent 1:2 or 1:3 complexes with ferrocenium cations[2,7]); alternatively they show metallic character (e.g., (TTF)(TCNQ)[45] or (TSeF)(TCNQ)[46]), as reported in excellent review articles concerning conducting organic compounds.[47,48] On the other hand, compounds with interesting magnetic properties (normal paramagnets, metamagnets,[29,31] but also low-temperature ferromagnets[32,35,49]) have been found.

The two 1,1′-bis(alkylthio)octamethylferrocenes **1** and **2** differ only in the steric bulk of the thioalkyl group and have the same redox potential of −0.28(2) V vs the Fc/Fc^+ couple, which corresponds also to the potential of the acceptor TCNQ.[4,29] Moreover, the redox potential of the trithiaferrocenophane **3** is higher (−0.10(2) V vs the Fc/Fc^+ couple) and the molecule is more compact, as compared to compounds **1** and **2**. Therefore, on the basis of these properties, different stoichiometries of the CT complexes were anticipated. Furthermore, for a more reliable interpretation of the magnetic properties of such CT complexes and because ferrocenes are known to have strongly anisotropic *Landé-g* factors,[50,51] six trihalogenide salts (with bromine and iodine) of **1**−**3**, possessing a paramagnetic cation and a diamagnetic anion, have been prepared. Magnetic susceptibility measurements thereof allowed the calculation of the ⟨*g*⟩-factors for the three ferrocene donor molecules **1**−**3**.

Results and Discussion

Synthesis of Charge-Transfer Complexes. The CT complexes **4** and **5** containing the octamethylferrocene derivatives **1** and **2**, respectively, and TCNQ could be obtained on mixing hot acetonitrile solutions of the two components, followed by slow cooling to room temperature. Even when the precursors were mixed in different ratios, only one stoichiometry of donor and acceptor was obtained, i.e., $[\mathbf{1}]_3[TCNQ]_7$ for **4** and $[\mathbf{2}][TCNQ]_3$ for **5**, as confirmed by elemental analyses on crystalline materials. Experiments using molar ratios of the reagents different from the stoichiometric coefficients of the CT salts afforded the products in lower yields and often contaminated by the neutral starting materials. A ratio of donor and acceptor of 3:7, as observed for **4** is unprecedented in the solid-state chemistry of TCNQ.

The third CT complex **6**, $[\mathbf{3}][TCNQ]_2$, could only be obtained upon addition of an excess of $[Bu_4N]BF_4$ to the reaction mixture. Black crystals of **6** were thus obtained in good yields by slow evaporation of solutions at ca. 60 °C during several days. In the absence of $[Bu_4N]BF_4$ only the neutral starting materials crystallized.

(22) Lequan, R. M.; Lequan, M.; Flandrois, S.; Delhaes, P.; Bravic, G.; Gaultier, J. *Synth. Met.* **1991**, *42*, 1663−1666.
(23) Bravic, G.; Gaultier, J.; Chasseau, D.; Lequan, R. M.; Lequan, M. *Acta Crystallogr.* **1992**, *48C*, 1425−1428.
(24) Bolinger, C. M.; Darkwa, J.; Gammie, G.; Gammon, S. D.; Lyding, J. W.; Rauchfuss, T. B.; Wilson, S. R. *Organometallics* **1986**, *5*, 2386−2388.
(25) Pasynskii, A. A.; Eremenko, I. L.; Porai-Koshits, M. A.; Katser, S. B.; S., A. A.; Aliev, A. S.; Katugin, A. S.; Orazsakhatov, B.; Okhlobystin, O. Y.; Privalov, V. I. *Metalloorg. Khim. (Organomet. Chem. in USSR)* **1990**, *3*, 454−461.
(26) Baird, P.; Bandy, J. A.; Green, M. L. H.; Hamnet, A.; Marseglia, E.; Obertelli, D. S.; Prout, K.; Qin, J. *J. Chem. Soc., Dalton Trans.* **1991**, 2377−2393.
(27) Bell, S. E.; Field, J. S.; Haines, R. J. *J. Chem. Soc., Chem. Commun.* **1991**, 489−491.
(28) Willi, C.; Reis, A. H.; Gebert, E.; Miller, J. S. *Inorg. Chem.* **1981**, *20*, 313−318.
(29) Miller, J. S.; Zhang, J. H.; Reiff, W. M.; Dixon, D. A.; Preston, L. D.; Reis, A. H.; Gebert, E.; Extine, M.; Troup, J.; Epstein, A. J.; Ward, M. D. *J. Phys. Chem.* **1987**, *91*, 4344−4360.
(30) Miller, J. S.; Gebert, E.; Reis, A. H.; Ritsko, J. J.; Salaneck, W. R.; Kovnat, L.; Cape, T. W.; Van Duyne, R. P. *J. Am. Chem. Soc.* **1979**, *101*, 7111−7113.
(31) Reis, A. H.; Preston, L. D.; Williams, J. M.; Peterson, S. W.; Candela, G. A.; Swartzendruber, L. J.; Miller, J. S. *J. Am. Chem. Soc.* **1979**, *101*, 2755−2758.
(32) Broderick, W. E.; M., E. D.; Liu, X.; Toscano, P. J.; Owens, S. M.; Hoffmann, B. M. *J. Am. Chem. Soc.* **1995**, *117*, 3641−3642.
(33) Dixon, D. A.; Calabrese, J. C.; Miller, J. S. *J. Phys. Chem.* **1989**, *93*, 3, 2284−2291.
(34) Wang, X.; Liable-Sands, L. M.; Manson, J. L.; Rheingold, A. L.; Miller, J. S. *J. Chem. Soc., Chem. Commun.* **1996**, 1979−1980.
(35) Broderick, W. E.; Thompson, J. A.; Day, E. P.; Hoffmann, B. M. *Science* **1990**, *249*, 401−403.
(36) Miller, J. S.; Glatzhofer, D. T.; O'Hare, D. M.; Reiff, W. M.; Chakraborty, A.; Epstein, A. J. *Inorg. Chem.* **1989**, *28*, 2930−2939.
(37) Chi, K. M.; Calabrese, J. C.; Reiff, W. M.; Miller, J. S. *Organometallics* **1991**, *10*, 688−693.
(38) Stein, D.; Sitzmann, H.; Boese, R.; Dormann, E.; Winter, H. *J. Organomet. Chem.* **1991**, *412*, 143−155.
(39) Stein, D.; Sitzmann, H.; Boese, R. *J. Organomet. Chem.* **1991**, *421*, 275−283.
(40) Wilson, S. R.; Corvan, P. J.; Seiders, P. J.; Hodgson, D. J.; Brookhart, M.; Hatfield, W. E.; Miller, J. S.; Reis, A. H.; Rogan, P. K.; Gebert, E.; Epstein, A. J. In *Molecular Metals*; Hatfield, W. E., Ed.; Plenum: New York, 1979; Vol. 6, pp 407−414.
(41) Murphy, V. J.; O'Hare, D. *Inorg. Chem.* **1994**, *33*, 1833−1841.
(42) Ward, M. D.; Johnson, D. C. *Inorg. Chem.* **1987**, *26*, 4213−4227.
(43) O'Hare, D.; Ward, M. D.; Miller, J. S. *Chem. Mater.* **1990**, *2*, 758−763.
(44) Atwood, D. A.; Cowley, A. H.; Dennis, S. M. *Inorg. Chem.* **1993**, *32*, 1527−1528.
(45) Ferraris, J. F.; Cowan, D. O.; Walatka, V.; Perlstein, J. H. *J. Am. Chem. Soc.* **1973**, *95*, 948−949.
(46) Engler, E. M.; Patel, V. V. *J. Am. Chem. Soc.* **1974**, *96*, 7376−7377.
(47) Bryce, M. R. *Chem. Soc. Rev.* **1991**, *20*, 355−390.
(48) Torrance, J. B. *Acc. Chem. Res.* **1979**, *12*, 79−86.
(49) Broderick, W. E.; Hoffmann, B. M. *J. Am. Chem. Soc.* **1991**, *113*, 6334−6335.
(50) Miller, J. S.; Calabrese, J. C.; Rommelmann, H.; Chittipeddi, S. R.; Zhang, J. H.; Reiff, W. M.; Epstein, A. J. *J. Am. Chem. Soc.* **1987**, *109*, 769−781.
(51) Duggan, D. M.; Hendrickson, D. N. *Inorg. Chem.* **1975**, *14*, 955−970.

Table 1. Crystallographic Data for CT Complexes 4, 5, 7, and 9

	4	5	7	9
formula	$C_{48}H_{39.33}N_{9.33}S_2Fe$	$C_{31}H_{27}N_6SFe_{0.5}$	$C_{32}H_{30}F_4N_4S_2Fe$	$C_{30}H_{24}F_4N_4S_3Fe$
fw	866.86	543.6	666.57	668.57
cryst dimens, mm	0.2 × 0.3 × 0.3	0.2 × 0.4 × 0.4	0.4 × 0.4 × 0.8	0.36 × 0.22 × 0.2
cryst syst	triclinic	triclinic	triclinic	triclinic
space group (No.)	$P\bar{1}$ (No. 2)	$P\bar{1}$ (No. 2)	$P\bar{1}$ (No. 2)	$P\bar{1}$ (No.2)
a, Å	8.860(4)	8.834(9)	8.780(3)	9.6858(15)
b, Å	16.375(8)	10.173(9)	14.716(4)	11.951(2)
c, Å	23.199(12)	17.12(2)	24.879(9)	25.199(4)
α, deg	81.56(2)	82.36(7)	81.98(3)	102.17(3)
β, deg	80.72(2)	83.34(8)	87.89(3)	91.91(3)
γ , deg	84.69(2)	68.20(8)	79.24(2)	92.02(3)
V, Å^3	3278(3)	1412(2)	3127(2)	2847.1(8)
Z	3	2	4	4
ρ(calcd)$_r$, g cm^{-3}	1.318	1.278	1.416	1.560
μ, mm^{-1}	0.486	0.392	0.668	0.805
F(000)	1352	568	1376	1368
diffractometer	Syntex P21	Syntex P21	Syntex P21	Siemens SMART PLATFORM with CCD detector
wavelength *λ*, Å	Mo Kα, $\lambda = 0.71073$	Mo Kα, $\lambda = 0.71073$	Mo Kα, $\lambda = 0.71073$	Mo Kα, $\lambda = 0.71073$
θ range, deg	1.64−20.06	2.58−20.04	1.54−20.04	0.83−26.40
no. of measd reflcns	6714	2832	5878	21370
no. of obsd reflcns (*n*)[a]	6178	2611	5878	11625
no. of params refined (*p*)	818	350	776	762
wR2 [$I > 2\sigma(I)$][b]	0.0690	0.0965	0.1104	0.0947
R1 [$I > 2\sigma(I)$][c]	0.0328	0.0350	0.0455	0.0421
GOF on F^2 [d]	0.737	1.091	0.888	0.926

[a] ($|F_o^2| > 4.0\sigma(|F|^2)$). [b] wR2 = $[\sigma(w(F_o^2 - F_c^2)^2]/\sigma[w(F_o^2)^2]^{1/2}$. [c] R1 = $\sigma||F_o| - |F_c||/\sigma|F_o|$. [d] GOF = $S = [\sigma(w(F_o^2 - F_c^2)^2]/(n - p)]^{1/2}$.

Table 2. Crystallographic Data for Compounds 11, 12, 14, and 15

	11	12	14	15
formula	$C_{26}H_{42}FeBr_3S_2$	$C_{18}H_{24}FeBr_3S_3$	$C_{26}H_{42}FeI_3S_2$	$C_{18}H_{24}FeI_3S_3$
fw	740.30	632.13	855.27	733.13
cryst dimens, mm	1.2 × 0.2 × 0.1	0.2 × 0.15 × 0.12	0.3 × 0.1 × 0.1	0.3 × 0.3 × 0.1
cryst syst	monoclinic	triclinic	orthorhombic	orthorhombic
space group (No.)	$P2_1/n$ (No. 14)	$P\bar{1}$ (No. 2)	*Pnnm* (No. 58)	*Pbca* (No. 61)
a, Å	10.572(3)	9.194(5)	10.878(6)	15.189(9)
b, Å	10.928(4)	11.104(6)	11.003(7)	12.610(7)
c, Å	13.533(5)	12.092(6)	13.533(7)	25.080(15)
α, deg	90	76.64(2)	90	90
β, deg	94	79.310(10)	90	90
γ , deg	90	69.64(2)	90	90
V, Å^3	1559.3(9)	1118.5(10)	1620(2)	4804
Z	2	2	2	8
ρ(calcd)$_r$, g cm^{-3}	1.521	1.877	1.754	2.138
μ, mm^{-1}	4.474	14.294	3.466	4.746
F(000)	722	622	830	2920
diffractometer	Syntex P21	Syntex P21	Syntex P21	Syntex P21
wavelength *λ*, Å	Mo Kα, $\lambda = 0.71073$	Mo Kα, $\lambda = 0.71073$	Mo Kα, $\lambda = 0.71073$	Mo Kα, $\lambda = 0.71073$
θ, range, deg	2.36−20.04	1.89−25.00	2.39−22.55	1.62−22.55
no. of measd reflcns	1461	2287	1126	3166
no. of obsd reflcns (*n*)[a]	1461	2287	1126	3166
no. of params refined (*p*)	156	227	92	227
wR2 [$I > 2\sigma(I)$][b]	0.0871	0.1274	0.0601	0.1485
R1 [$I > 2\sigma(I)$][c]	0.0390	0.0491	0.0265	0.0579
GOF on F^2 [d]	0.750	1.092	0.727	0.838

[a] ($|F_o^2| > 4.0\sigma(|F|^2)$). [b] wR2 = $[\sigma(w(F_o^2 - F_c^2)^2]/\sigma[w(F_o^2)^2]^{1/2}$. [c] R1 = $\sigma||F_o| - |F_c||/\sigma|F_o|$. [d] GOF = $S = [\sigma(w(F_o^2 - F_c^2)^2]/(n - p)]^{1/2}$.

The three corresponding CT salts containing $TCNQF_4$, **7**−**9**, were obtained by a similar procedure as applied for **4** and **5**. However, only the 1:1 stoichiometry was observed, even when an excess of $TCNQF_4$ was used. Finally, the six trihalogenide salts **10**−**15**, [Donor][X_3] (see Scheme 1), could be obtained by simply adding a slight excess of halogen to the corresponding ferrocene in 1,2-dichloroethane. Slow diffusion of *tert*-butylmethyl ether into these solutions afforded the crystalline products in yields up to 88%.

Solid-State Structure of Charge-Transfer Complexes. In view of the different stoichiometries observed for CT complexes containing structurally related donors and acceptors, and in order to understand their physical properties (vide infra), it was important to elucidate the factors so drastically influencing the composition of the crystalline materials. Single crystals suitable for X-ray diffraction studies were obtained for compounds **4**, **5**, **7**, **9**, **11**, **12**, **14**, and **15**. Tables 1 and 2 gives the relevant crystal and data collection parameters. Bond distances and angles of each asymmetric unit were found to fall in the expected ranges and will not be discussed here (they are provided as Supporting Information, along with ORTEP representations of the respective asymmetric unit). Figures 1−7 illustrate the relative arrangement of the molecular components in tridimensional space.

Crystals of **4**, **5**, **7**, and **9** are triclinic and belong to

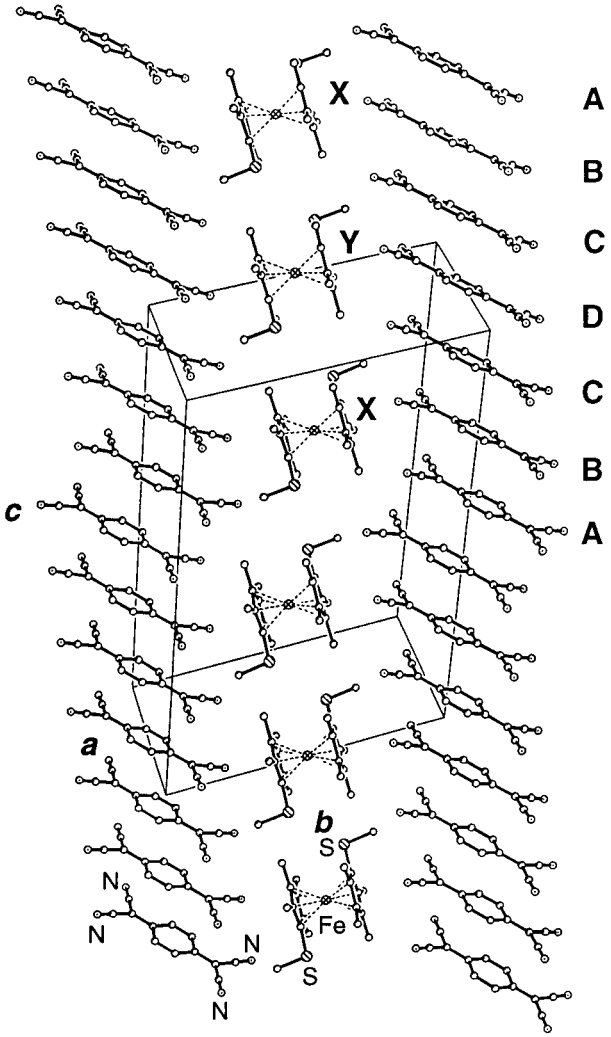

Figure 1. Side view of two TCNQ stacks flanking one column of ferrocenium cations in **4**. The steric demand of the three cations **XYX** along the stack is very similar to the length of a group of seven TCNQ molecules.

space group $P\bar{1}$. $[Fe(\eta^5\text{-}C_5Me_4SMe)_2]_3(TCNQ)_7$ (**4**) shows alternating layers of TCNQ stacks and ferrocenium columns. The TCNQ molecules form regular stacks, each interrupted after seven units by a sharp bend. A side view of two stacks of TCNQ and a ferrocenium column is shown in Figure 1.

There are four crystallographically independent acceptor molecules **A**−**D** arranged in the order **ABCDBCA** in a row of seven units, whereby **D** lies on a symmetry center. Within each group of seven TCNQ's the centers of gravity of the seven molecules lie on a straight line. This is illustrated by the angles of 179° between the centers of the acceptors **ABC** and **BCD**, respectively. The plane defined by any of the seven TCNQ molecules forms an angle of 58° with this axis. The distance between the centers of the TCNQ's lies between 3.87 and 3.89 Å. The bend of the TCNQ stacks is characterized by an angle of 142° between the axes of two groups of seven molecules. The distance between the centers of two neighboring molecules **A** is 3.53 Å. Thus, the two **A** molecules are shifted by only 0.79 Å in the direction of the longer molecular axes, whereas for the other pairs (**AB**, **BC**, **CD**) this shift is 2.07. The distances between the planes of the TCNQ moieties are between 3.25 Å for **BC** and 3.30 Å for **AB**. This is what

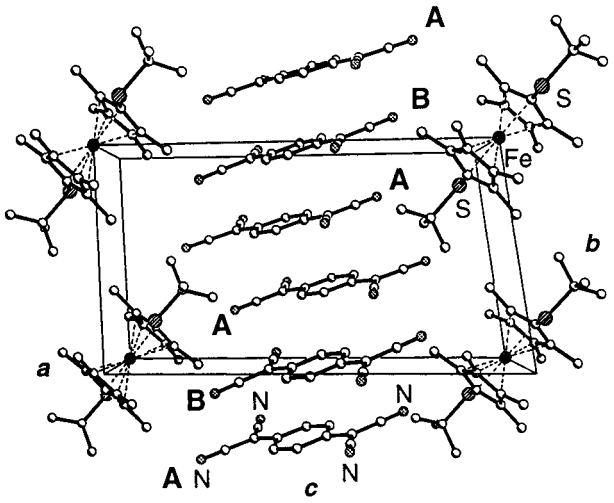

Figure 2. Side view of two ferrocenium columns with one TCNQ stack shifted to the front of them in **5**. The steric demand of one cation along the stack is very similar to the length of a group of three TCNQ molecules.

is expected for van der Waals stacking of aromatic rings and what is observed also for other CT complexes with TCNQ.[18,19,27,52] The molecular planes are almost parallel, with interplanar angles of 0.3° for **BC** and 3.30° for **AB**. There are two crystallographically independent ferrocenium cations, **X** and **Y**, the iron atom of the latter being placed on a symmetry center. Thus, the iron centers of the three cations **XYX** form a perfect straight line. The distance Fe^X-Fe^Y is 8.43 Å, the corresponding distance between neighboring molecules (Fe^X-Fe^X) is 9.49 Å, and the angle $Fe^XFe^XFe^Y$ is 164.4°. The shortest Fe−Fe distance between two columns is 8.86 Å, corresponding to the cell dimension *a*. The pseudo-centrosymmetric cation **X** has two parallel Cp rings (interplanar angle 0.7°), which are rotated against each other by 178°.

$[Fe(\eta^5\text{-}C_5Me_4S^tBu)_2](TCNQ)_3$ (**5**) is characterized by alternating layers of TCNQ stacks and ferrocenium columns, and the general features of its structure are very similar to those of $[Fe(\eta^5\text{-}C_5Me_4SMe)_2]_3(TCNQ)_7$ (**4**). The difference is found in the stoichiometry of 1:3 for **5** instead of 3:7 for **4**. A TCNQ stack between two ferrocenium columns is shown in Figure 2.

There are two crystallographically independent TCNQ units **A** and **B**, with **B** on a symmetry center. Always three molecules form a group with the respective centers of gravity on a straight line and a distance between the centers of 3.97 Å. The two acceptors **A** and **B** are shifted by 2.20 Å and the two neighboring molecules **A** by 1.32 Å in the direction of the longer molecular axes. The angle between the centers of the molecules **AAB** is 131° and the associated distance between two neighboring units **A** is 3.68 Å. The interplanar distance of the TCNQ units is 3.30 Å between **AB** and 3.44 Å between **AA**. The interplanar angle of **A** and **B** is 2°. The ferrocenium cations are placed on the symmetry centers in the edges of the elementary cell. The Fe−Fe distance in the stacking direction corresponds to the diagonal of the *ab* plane (10.71 Å), and the shortest Fe−Fe distance corresponds to the cell axis *a* (8.83 Å).

(52) Ward, M. D.; Calabrese, J. C.; Fagan, P. J. *J. Am. Chem. Soc.* **1989**, *111*, 1698−1719.

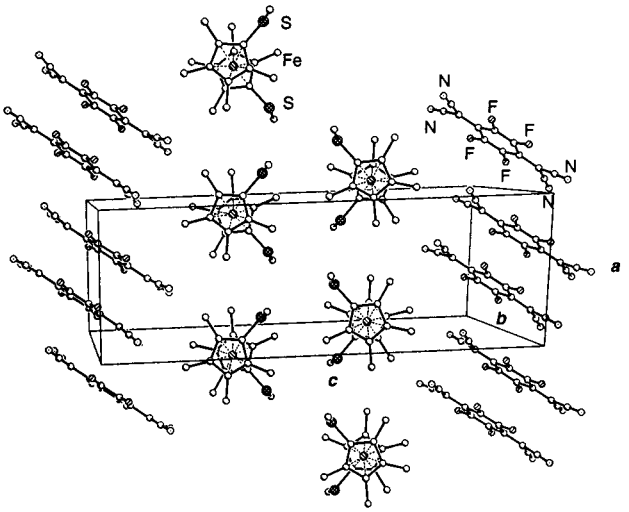

Figure 3. Side view of two $TCNQF_4$ stacks with two ferrocenium columns in **7**. The anions form dimers with an interplanar distance of 3.16 Å.

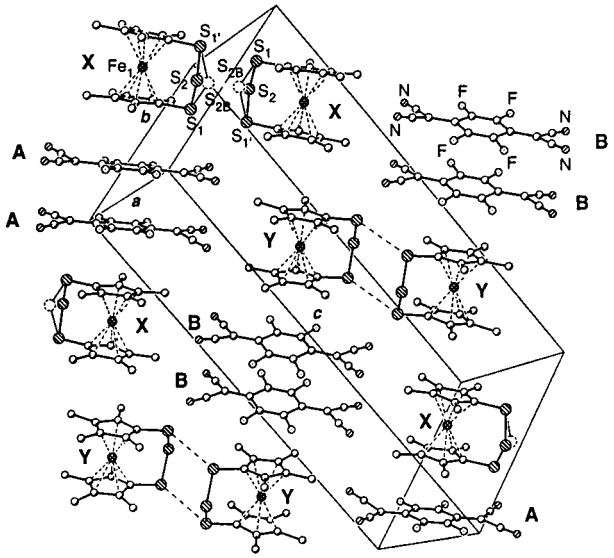

Figure 4. View of a layer of three stacks in **9**. The crystallographic independent molecules are marked with **A** and **B**, or **X** and **Y,** respectively.

In $[Fe(\eta^5\text{-}C_5Me_4SMe)_2](TCNQF_4)$ (**7**) the ferrocenium ions form two columns surrounded by four stacks of $TCNQF_4$. The structure is quite similar to that of $[Fe(\eta^5\text{-}C_5Me_4SMe)_2][Ni(mnt)_2]$.[1] The $TCNQF_4$ anions form dimers, within which the single units are shifted against each other by 1.1 Å along the main molecule axis with an interplanar distance of 3.16 Å. This is shorter than what is expected for a van der Waals distance and also shorter than in the 1:1 charge-transfer complex with ferrocene (3.23 Å),[20] where segregated stacks of $TCNQF_4$ and ferrocenium cations are observed. Therefore, an attractive interaction between these two anions must be operating. The interdimer distance is slightly larger (3.42 Å), but also shorter than in the above-mentioned ferrocenium complex (3.67 Å). Two neighbored dimers are shifted parallel to the ring plane by 5.10 Å with respect to one another. This leads to a zigzag arrangement along the centers of the anions with alternating long (6.15 Å) and short (3.34 Å) distances. A side view of two stacks of $TCNQF_4$ anions with two ferrocenium colums between them is shown in Figure 3.

Like in the corresponding $[Ni(mnt)_2]$ salt,[1] the symmetry of the cation is C_1. The two Cp planes are almost parallel, with an interplanar angle of 1°, and are rotated against each other by 98°. The Fe−Fe distance along the stacking direction is 8.78 Å (unit cell axis *a*) and 8.44 Å perpendicular to the columns. The shortest S−S distance is 3.94 Å between two ferrocenes in a column.

In contrast to the three structures above, in $[Fe(\eta^5\text{-}C_5Me_4S)_2S](TCNQF_4)$ (**9**) no segregated stacks of anions and cations are observed. The structure is best described by a $D^+D^+A^-A^-D^+D^+A^-A^-$ motif, which can be compared to what is found in crystals of $[Fe(\eta^5\text{-}C_5HEt_4)_2](TCNQF_4)$.[39] There are two crystallographically independent ferrocenophanium molecules **X** and **Y** as well as two different $TCNQF_4$ molecules **A** and **B**. The order of the molecules in an alternating stack is $D_{\mathbf{X}}{}^+D_{\mathbf{Y}}{}^+\text{-}A_{\mathbf{B}}{}^-A_{\mathbf{B}}{}^-D_{\mathbf{Y}}{}^+D_{\mathbf{X}}{}^+A_{\mathbf{A}}{}^-A_{\mathbf{A}}{}^-$, and so forth, with a symmetry center located between two acceptor molecules. A view of the structure of **9** is illustrated in Figure 4.

The relative arrangement of the molecules is such that one acceptor dimer is almost completely surrounded by ferrocenophanium cations. The middle sulfur atom of the cation **X** was found to be disordered and occupying two different positions (S_2 und S_{2B}). Position S_{2B} has an occupancy of only 10%, which corresponds to an electron density of about two electrons. Thus, it is very unlikely that this position (S_{2B}) is occupied at the same time in two neighbored molecules, such that the distance of 2.24 Å between such two S_{2B} atoms is irrelevant. However, the distance between an atom in position S_{2B} and a sulfur atom S_1 in a neighboring molecule is very short (3.21 Å), possibly indicating at least a weak attractive interaction between these two cations. Similarly, the cations **Y** form a unit with quite a short intermolecular S−S distance of 3.63 Å (S_1 positions). The sulfur atoms of such a unit can be viewed as forming a six-membered ring assuming a chairlike conformation. The interplanar distances between acceptor molecules within the dimers are quite similar (3.17 Å for **A**−**A** and 3.15 Å for **B**−**B**). Also the shift of one molecule with respect to the other, parallel to the respective planes and perpendicular to the longer molecular axis, is 0.57 Å for **A**−**A** and 0.71 Å for **B**−**B**. However, there are important differences between the two acceptor dimers that are worth noting. The six-membered rings in dimer **A** are almost parallel (interplanar angle of 3°); a more significant deviation from this situation is observed in dimer **B**, with an interplanar angle of 10°. Whereas the $TCNQF_4$ units **A** are as expected almost planar, the corresponding units **B** are not. The planar exocyclic dicyanomethylene groups in **B** are rotated by 11° with respect to the plane of the six-membered ring, this probably being due to steric reasons. A similar but more pronounced distortion of this kind (with an angle of 33°, as mentioned) has been observed for the $TCNQF_4{}^{2-}$ dianion in the 2:1 CT complex with decamethylferrocene reported by Miller and co-workers.[33] In contrast, in **A** only two of the four nitrile groups lie slightly out of the plane defined by the six-membered ring and the four fluorine atoms. The distance of the nitrogen atoms from this plane, however, is less than 0.5 Å.

$[Fe(\eta^5\text{-}C_5Me_4S^tBu)_2](Br_3)$ (**11**) crystallizes in the mono-

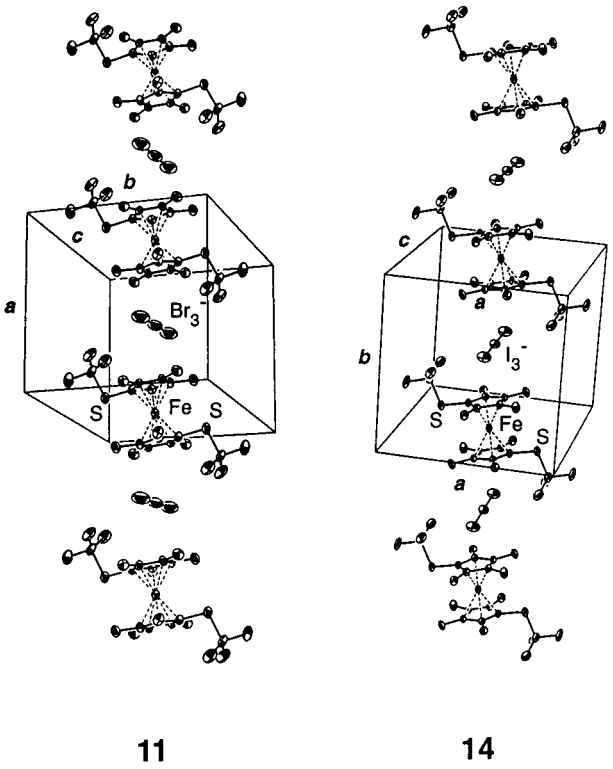

Figure 5. Comparison of the two similar structures of **11** and **14** (thermal ellipsoids are drawn at the 50% probability level at 293 K).

clinic space group $P2_1/n$ with one ferrocenium cation and one tribromide anion on a symmetry center. The anions and cations are alternating along the cell axes *a*. The middle bromine atom and the carbon atoms C(3) and C(4) of the Cp ring are very close (3.55 and 3.58 Å, respectively). Alternating stacks of compound **11** and its very similar companion **14**, ([Fe(η^5-$C_5Me_4S^tBu)_2$](I_3)), are depicted in Figure 5.

However, as opposed to **14**, (vide infra) the Br_3 anion is not parallel to the Cp ring; thus three different distances of the three bromine atoms to the Cp plane are observed (3.08 Å for Br(1), 3.49 Å for Br(2), and 3.89 Å for Br(1′)). On the other hand, in **14**, which crystallizes in the orthorhombic space group *Pnnm*, the ferrocenium cation and the triiodide simultaneously lie on a symmetry plane and coincide with a symmetry center. Also in this case, the distance of the middle halide atom to the carbon atom C(3) of the Cp ring is quite short (3.77 Å), and the distance to the plane of the Cp ring is 3.70 Å. In both cases, the outer halide atoms display short distances to proximate methyl groups of 3.51 and 3.52 Å for **11** and 4.10 and 4.11 Å for **14**, respectively. The distance of the two iron atoms along the stack is for both compounds very similar (**11**, 10.57 Å; **14**, 11.0 Å).

[Fe(η^5-$C_5Me_4S)_2S$](Br_3) (**12**) crystallizes in the triclinic space group $P\bar{1}$ with the anion and the cation in general positions. The most interesting structural feature is that two Br_3^- units together form a chain with ends on both sides with an S_3 bridge of a cation. A projection of the elementary cell and two such chains is depicted in Figure 6.

The shortest S−Br distance is 3.66 Å, and the Br−Br distance between two anions is 3.59 Å. The latter are almost parallel (the angle between them is 1°), however not collinear, and the Br−Br distances within

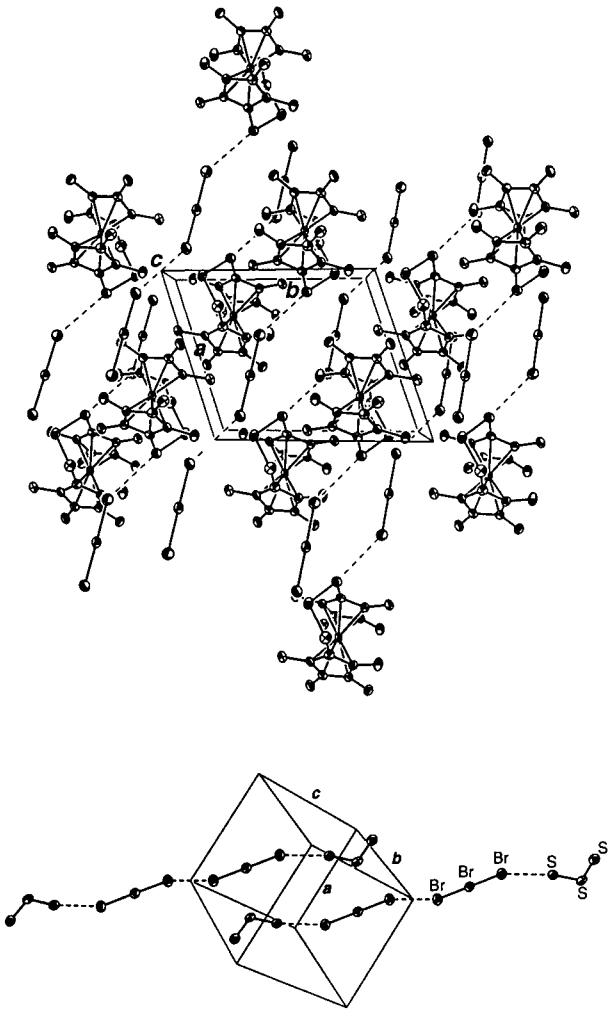

Figure 6. Projection of the elementary cell of **11** along *c* (top), and illustration of two $S_3(Br_3)_2S_3$ chains (bottom, thermal ellipsoids are drawn at the 50% probability level at 293 K).

an anion are very similar (2.51 and 2.57 Å). Finally, the Cp rings in the ferrocenophanium are eclipsed with an interplanar angle of 4.4°.

Crystals of [Fe(η^5-$C_5Me_4S)_2S$](I_3) (**15**) are orthorhombic (space group *Pbca*) with the cation and the anion in general positions. Along the cell axis *c*, one observes layers containing ferrocenophanium cations and triiodide anions. Zigzag chains of triiodide anions are connected by the three sulfur atoms of the ferrocenophanium, thus forming a two-dimensional network with shortest S−I distances of 3.80 and 3.76 Å. Such a network, a view of which is provided in Figure 7, may also be described as a net of intersecting S_3I_4 chains, with the Fe($C_5Me_4)_2$ units filling the gaps between the chains (such as balls caught in a wire-mesh).

The I−I distance between the anions is 3.95 Å, and the angle between the two triiodides is 80°. The anions are not perfectly linear but slightly bent with an I−I−I angle of 176.7°. Finally, the two different I−I distances in each anion are 2.87 and 3.00 Å, and the angle between the planes of the eclipsed Cp rings is 4.5°.

Infrared Spectroscopy. For the three CT complexes with TCNQ (**4**−**6**), IR spectra quite typical for semiconductors are observed. Thus, above 1600 cm^{-1} for **4** and **5** and above about 1000 cm^{-1} for **6**, the three compounds

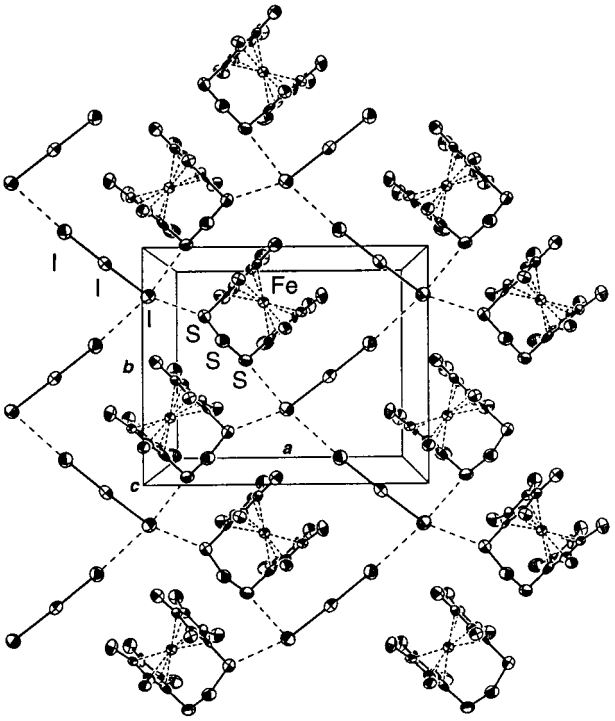

Figure 7. Projection of a layer of **15** along *c*. The triiodide anions and the sulfur bridges form a two-dimensional network (thermal ellipsoids are drawn at the 50% probability level at 293 K).

are opaque. Because the measurement was done at room temperature, no sharp absorption edge but only a "round" transition was observed. The band gaps determined by a temperature-dependent resistivity measurement (see below) confirm the interpretation of the infrared spectra. On the other hand, the three $TCNQF_4$ salts (**4**−**9**) are transparent in the whole measured range of 250−4400 cm^{-1}, in agreement with their insulator behavior. The CN stretching vibrations are observed at 2194 and 2175 cm^{-1} for **7**, at 2192 and 2170 cm^{-1} for **8,** and at 2195 and 2177 cm^{-1} for **9**, values very similar to those reported in the literature.[20] The six trihalogenide salts do not show any exceptional features in the infrared spectra.

Conductivity Measurements. For the three semiconducting compounds (**4**−**6**), temperature-dependent two-point resistivity measurements were carried out on pressed pellets. The room-temperature conductivities are in the range of about 0.1−0.3 S cm^{-1} for **4** and **5** to 3.4 S cm^{-1} for **6**. A plot ot the natural logarithm of the conductivity ($1/R$) vs the reciprocal temperature ($1/T$) is depicted in Figure 8.

The semiconductor nature of **4** and **5** is made plausible by their structural features. The acceptor stacks are responsible for the conductivity, whereas the ferrocenes serve as spacers and as electron reservoirs. The sharp bends in the TCNQ stacks after seven or three units, respectively, lead to a band gap at the Fermi level. They possibly could be attributed to Peierls distortion,[53] although experiments aimed at proving this have not been performed. The temperature dependence of the resistivity of **4** obeys the equation of a semiconductor only above 250 K[54−56] (eq 1), with a band gap of about

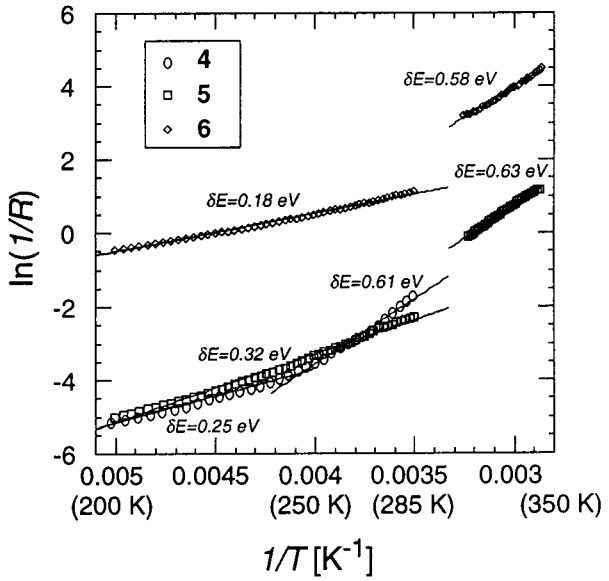

Figure 8. $\ln(1/R)$ vs $(1/T)$ plot for the three TCNQ compounds **4**−**6** in the temperature range 200−350 K. The straight lines are linear regressions leading to the energy gap δE in the corresponding temperaure range.

0.60 eV (∼4900 cm^{-1}) and a room-temperature conductivity of 0.26 S cm^{-1}.

$$1/R = (1/R)_0\, e^{-\delta E/(2kT)} \qquad (1)$$

Below 250 K there is a fast decrease of the slope in the $\ln(1/R)$ vs $(1/T)$ plot, and in the range between 200 and 250 K the activation energy (δE) is only 0.25 eV. This effect can tentatively be explained by localized structural defects, similar to what is found for a doped semiconductor, and from which empty energy levels between the valence and the conduction band arise. However, more detailed studies would be needed in order to fully characterize the observed conductivity behavior.

The room-temperature conductivity of **5** is smaller (0.1 S cm^{-1}) than that of **4**, although its behavior is very similar to that of **4** with a band gap of 0.32 eV (∼2600 cm^{-1}) in the temperature range of 200−285 K. By heating the compound to 350 K, the activation barrier increases to 0.63 eV (∼5000 cm^{-1}).

Compound **6,** whose solid-state structure is not known, displays a behavior similar to the former two compounds. However, the band gap in the temperature range of 200−285 K is smaller (0.18 eV (∼1600 cm^{-1})) and the room-temperature conductivity is more than 10 times larger (3.4 S cm^{-1}). An explanation of this could be the dendritic growth of the crystals, leading to a bad crystal quality of the material, thus producing a large number of structural defects. By heating the compound to 350 K, again the activation energy increases to 0.58 eV (∼4700 cm^{-1}).

Magnetic Measurements. Magnetic susceptibility measurements were carried out for the 12 compounds **4**−**15** using a SQUID susceptometer in the temperature

(53) Peierls, R. E. *Quantum Theory of Solids*; Oxford University Press: Oxford, 1955.

(54) Wedler, G. *Lehrbuch der Physikalischen Chemie*; VCH: Weinheim, 1987; pp 722−725.

(55) Kortüm, G.*Lehrbuch der Elektrochemie*; Verlag Chemie: Weinheim, 1972; pp 258−261.

(56) Meier, H.*Organic Semiconductors*; Verlag Chemie: Weinheim, 1974; pp 39−71.

Table 3. Survey of Magnetic Data for Compounds 4−15

compd	Curie const. C [cm^3 K/mol]	Weiss const. θ [K]	J_{AA} [cm^{-1}]	J_{DD} [cm^{-1}]	$\langle g_D \rangle$	$q \times 10^{-6}$ [cm^3/mol]
4	0.65(2)	−1(1)				1609(79)
5	0.87(1)	−2.0(5)	−22(1)	+54(7)	2.48(2)	2520(45)
6	0.506(2)	0.0(1)	−920(67)	−0.56(3)	2.702(4)	2441(12)
7	0.67(1)	0(1)	>1000	0	3.07(1)	1043(63)
8	0.74(1)	+0.8(7)	>1000	+2.0(2)	3.28(1)	1235(44)
9	0.600(5)	−0.4(4)	>1000	−0.32(5)	2.901(3)	754(21)
10	0.458(3)	+3.4(4)			2.20	659(14)
11	0.526(3)	+0.6(3)			2.37	512(14)
12	0.61(1)	+0.6(12)			2.55	320(59)
13	0.61(1)	−0.8(8)			2.55	219(38)
14	0.531(7)	+0.3(6)			2.38	324(26)
15	0.490(6)	+0.4(6)			2.29	358(23)

range between 2 and 300 K and a constant external magnetic field of 1000 G. A survey of the fitted magnetic data is given in Table 3. All 12 compounds (**4**−**15**) obey a modified Curie−Weiss expression $\chi_{mol} = C/(T + \theta) + q$, where q is the sum of core diamagnetism and temperature-independent paramagnetism (TIP). For all compounds q is positive, meaning that χ_{TIP} is about twice the diamagnetic component χ_{Dia}, which can easily be calculated ($\chi_{Dia} = mM_r \times 10^{-6}$ cm^3 mol^{-1}, with m = 0.4−0.5).[57,58]

Because of their relative simplicity, the six trihalogenide salts **10**−**15** shall be discussed first. Except for the tribromide **10**, no significant interactions between the cations can be deducted (Weiss constants $\theta = 0$ K for **11**−**15**). However, in compound **10** a weak ferromagnetic interaction between the cations could be operating, as indicated by the slightly positive Weiss constant θ of 3.4(4) K, although no increase in the χT vs T plot was observed even below 10 K. Despite this observation, we conclude that the magnetic properties of these six compounds derive from the cations alone, therefore giving access to average *Landé-g* factors $\langle g_D \rangle$ for the three ferrocenium cations generated from **1**−**3** (Table 3). For the two cations from **1** and **3**, two different values are obtained for the tribromide and the triiodide salt, respectively. This can be explained by the different arrangement of the cations in the solid state. In the case of the trithiaferrocenophane **3** the structures of both compounds are known. In the tribromide salt **12** the cations are oriented all in the same direction, whereas in the triiodide salt **15** a pairwise arrangement of the cations, approximately orthogonal to each other, is observed. This different structural feature is probably responsible for the higher value of $\langle g_D \rangle$ in **12**, as compared to **15**. The two salts **11** and **14,** containing the cation from **3**, have more or less the same solid-state structure and thus the same $\langle g_D \rangle$-value. For the salts resulting from **1**, unfortunately no solid-state structure is known. The different $\langle g_D \rangle$-values indicate that the cations must have a different relative arrangement in the solid state. These results show that one should be very cautious in using *Landé-g* factors of anisotropic molecules to interpret magnetic susceptibility data, without knowing the structure of the compounds.

Plots of the reciprocal susceptibility $1/\chi_{mol}$ for the six compounds (**4**−**9**) and χ_{mol} vs T, respectively, are shown in Figures 9 and 10. [Fe(η^5-$C_5Me_4SMe)_2]_3(TCNQ)_7$ (**4**) has a Curie constant C of 0.65(2) cm^3 K mol^{-1} (μ_{eff} = 2.28, as obtained from high-temperature data according

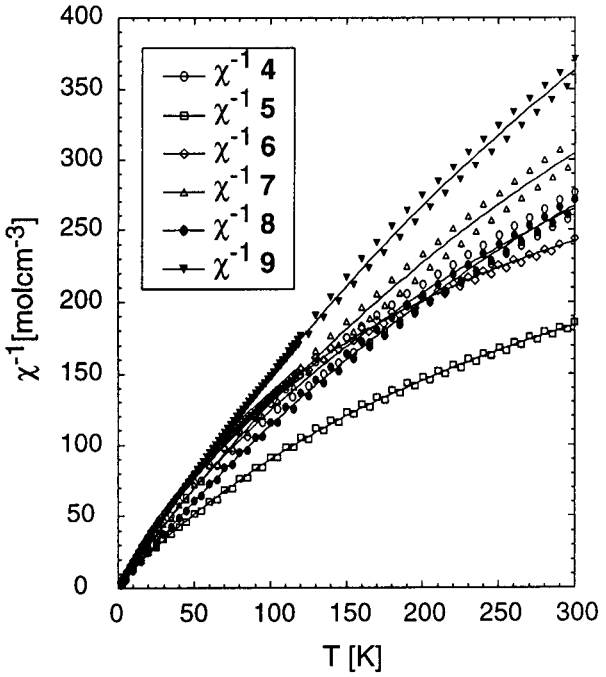

Figure 9. Reciprocal susceptibility data for the charge-transfer complexes **4**−**9**, measured in the temperature range of 2−300 K in an external field of 1000 G. The lines correspond to the best fit of the modified Curie−Weiss expression (see text).

to $\mu_{eff} = (3k\chi_{mol}T/N\beta^2)^{1/2}$), calculated per 1 mol of iron. In the case of a complete charge transfer from the ferrocenes to the acceptor, two unpaired electrons would result per ferrocenium/$(TCNQ)_{7/3}$ unit and a spin of $S = 2 \times 1/2$ should be expected. Thus, one would anticipate a Curie constant larger than 0.75 because the $\langle g_D \rangle$-value of the anisotropic ferrocenium cation should be larger than 2.0. One has to note that for decamethylferrocenium a $\langle g \rangle$-value of 2.8 ($g_{||} = 4.4$ and $g_\perp = 1.3$) was found by ESR spectroscopy.[50,51] Furthermore, from the magnetic data of [**1**][M(mnt)$_2$] (M = Ni, Co, Pt), $\langle g_D \rangle$-values between 2.0 and 3.2[1] were found (with $\langle g \rangle$-values for [M(mnt)$_2$]$^-$ known from the literature[59]), whereas for the tribromide and the triiodide salts of **1**,[60] $\langle g_D \rangle$-values of 2.20 and 2.55, respectively, were found (Table 3). From these values, a Curie constant between 0.75 and 1.3 can be calculated for **4**. This means that only 50−85% of the ferrocenes exist in the oxidized form in the solid state for this compound. From the length of

(57) Kahn, O. *Molecular Magnetism*; VCH: Weinheim, 1993.
(58) Epstein, A. J.; Miller, J. S. *Angew. Chem.* **1994**, *106*, 399−432.
(59) McCleverty, J. A. *Prog. Inorg. Chem.* **1968**, *10*, 50−215.
(60) Zürcher, S. Ferrocenhaltige molekulare Materialien. Ph.D. Thesis No. 12895, Eidgenössische Technische Hochschule (ETH), Zürich, 1998.

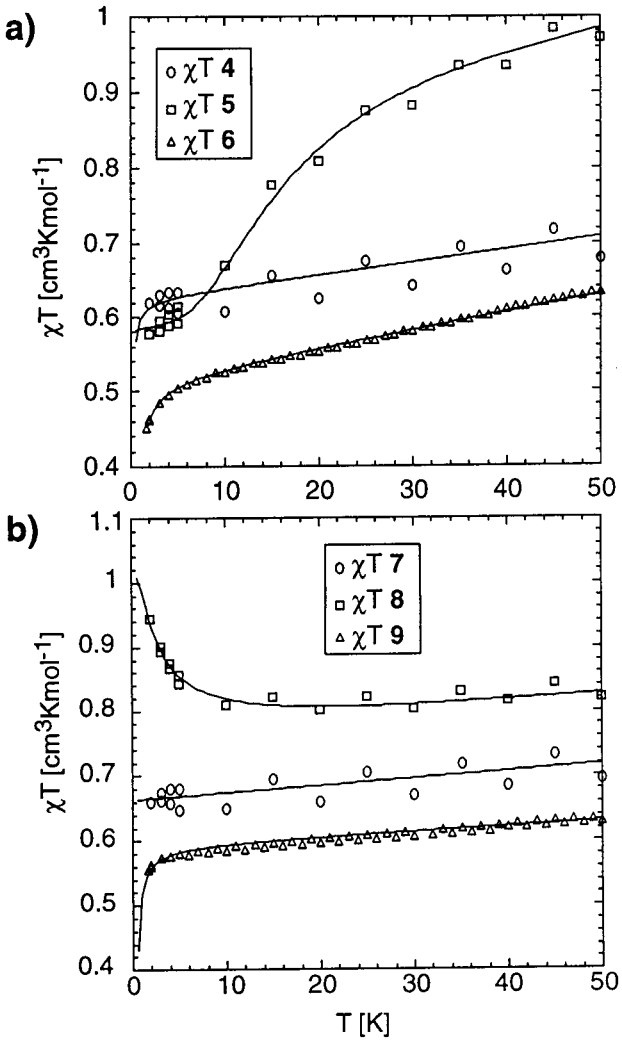

Figure 10. χT vs T plot for the six charge-transfer complexes **4**−**9**: for the three materials containing TCNQ (a) and for the three compounds containing $TCNQF_4$ (b). The lines correspond to the best fit according to eq 2.

the exocyclic double bond of the TCNQ anions the charge of the molecule can be inferred. The exocyclic double bonds of the seven TCNQ units have an average bond length of 1.39(1) Å (between 1.384(6) and 1.397(5) Å). This is closer to the value for $TCNQ^{1/2-}$ (1.390(3) and 1.394(4) Å)[28] than for the neutral TCNQ (1.374(4) Å).[61] Therefore, from both the magnectic data and structural parameters, we conclude that roughly two to three delocalized negative charges are associated with each seven-TCNQ unit, with the TCNQ molecules within such a unit being electronically equivalent. Finally, there is no significant coupling between the spins, as indicated by the linearity of the χT vs T plot of Figure 10 and a Weiss constant θ of −1(1) K.

The Curie constant C of $[Fe(\eta^5\text{-}C_5Me_4S^tBu)_2](TCNQ)_3$ (**5**) is 0.88 cm^3 K mol^{-1} (μ_{eff} = 2.65). This is only slightly less than what one would expect for an almost completely oxidized ferrocene and one negative charge per three TCNQ molecules. For the cation resulting from **2**, $\langle g_D \rangle$-values between 2.3 and 2.7 are observed from the magnetic properties of the corresponding $[M(mnt)_2]$ salts (M = Ni, Co, Pt),[1] whereas the magnetic data of the trihalogenide salts (Br_3 and I_3) of **2** afford $\langle g_D \rangle$-values of 2.37 and 2.38, respectively. A Curie constant between 0.9 and 1.1 cm^3 K mol^{-1} results, meaning that 80−100% of the ferrocene molecules are in the oxidized state. Again, the exocyclic double bonds of the three TCNQ fragments display an average bond length of 1.389(10) Å (between 1.383(4) and 1.392(4) Å). This is in good agreement with one negative charge per three TCNQ units. As opposed to **4**, however, **5** shows a small but significant antiferromagnetic coupling, as indicated by the negative Weiss constant θ of −1.9 ± 0.5 K. In the χT vs T plot (Figure 10a), a strong decrease below 50 K with a plateau at about 6 K is observed. This can be explained with antiferromagnetically coupled electrons on the TCNQ stacks (J_{AA} of −22(1) cm^{-1}) and ferromagnetically coupled electrons in the ferrocenium layers (J_{DD} of +54(7) cm^{-1}), with coupling constants resulting from a fitting of the data according to eq 2.

$$\chi = \frac{N\beta^2}{kT}\left(\frac{\langle g_D\rangle^2 S_D(S_D+1)}{3+e^{-J_{DD}/kT}} + \frac{\langle g_A\rangle^2 S_A(S_A+1)}{3+e^{-J_{AA}/kT}}\right) \quad (2)$$

$[Fe(\eta^5\text{-}C_5Me_4S)_2S](TCNQ)_2$ (**6**) displays a very small Curie constant C of 0.506(2) cm^3 K mol^{-1} (μ_{eff} = 2.01) and a Weiss constant θ of 0.0(1). In the χT vs T plot (Figure 10 a), a small decrease below 10 K is observed, whereas in the high-temperature range, the curve is not fully linear but slightly concave. By fitting the data with eq 2, a large negative coupling constant J_{AA} of −920(67) cm^{-1} turns out, meaning that there is a strong antiferromagnetic coupling of the negative charges associated with the TCNQ units. The decrease of the χT data below 10 K is explained by a weak antiferromagnetic interaction of the ferrocenium ions (J_{DD} = −0.56(3) cm^{-1}). Since no structural data are available for this compound, a more detailed interpretation of the magnetic data is not possible.

Because of the relatively large difference of the redox potentials of donor and acceptor, one would anticipate complete oxidations of the ferrocene molecules in **7** ($[Fe(\eta^5\text{-}C_5Me_4SMe)_2](TCNQF_4)$), concomitant with a Curie constant larger than 0.75 cm^3 K mol^{-1}. However, the strong dimerization in the anion stacks suggests a diamagnetic ground state (S = 0). Taking into account a $\langle g_D \rangle$-value of 2.5 and a spin S = 1/2, a value of the Curie constant C of 0.59 cm^3 K mol^{-1} results, which is only slightly below the measured value of 0.67(1) cm^3 K mol^{-1} (μ_{eff} = 2.32). A similar situation was reported for the 1:1 salts $[M(\eta^5\text{-}C_5Me_5)_2](TCNQF_4)$ (M = Fe, Co, Cr),[33] also containing S = 0 $(TCNQF_4)_2^{2-}$ dianions. A cooperative interaction of the remaining spins of the cations cannot be deduced, as indicated by the Weiss constant θ = 0(1) K and as it is also shown by the linear χT vs T plot of Figure 10 b).

The analogous complex $[Fe(\eta^5\text{-}C_5Me_4S^tBu)_2](TCNQF_4)$ (**8**) displays a slightly larger Curie constant (C = 0.75 cm^3 K/mol; μ_{eff} = 2.45), corresponding exactly to the theoretical value for an $S = 2 \times 1/2$ spin system ($\langle g_D \rangle$ = 2). Unfortunately, no structural data for this compound are available. However, the CN stretching vibrations of 2192 and 2170 cm^{-1} suggest that S = 0 $(TCNQF_4)_2^{2-}$ dianions are present. The relatively large value of C can be explained with the anisotropic $\langle g_D \rangle$-value of the cation. Below 10 K, an increase of χT in the χT vs T

(61) Long, R. E.; Sparks, R. A.; Trueblood, K. N. *Acta Crystallogr.* **1965**, *18*, 932−939.

plot is observed, indicating a small but significant ferromagnetic interaction ($J_{DD} = +2.0(2)$ cm^{-1}; Weiss constant $\theta = 0.8(7)$ K) between the ferrocenium cations.

Finally, a slightly different situation, however corroborated by structural data, is encountered for [Fe(η^5-$C_5Me_4S)_2S$](TCNQF$_4$) (**9**) (C 0.600(5) cm^3 K mol^{-1}, $\mu_{eff} = 2.19$, and θ of $-0.4(4)$ K). The crystal structure clearly shows that the compound contains diamagnetic $S = 0$ $(TCNQF_4)_2^{2-}$ dianions. Only a very small antiferromagnetic coupling between the donor molecules is observed ($J_{DD} = -0.32(5)$ cm^{-1}).

Conclusions

We have shown that the stoichiometry of charge-transfer salts of structurally related sulfur-containing ferrocene electron donors with the acceptor TCNQ very much depends on the relative size and orientation of the two components in the solid state. Thus, for example, the unusual donor−acceptor ratio of 3:7 for compound **4** derives from an almost ideal fit, in terms of shape and volume, of a row of three ferrocenes **1** with a stack of 7 TCNQ's. On the other hand, the higher reduction potential of $TCNQF_4$, combined with its strong tendency to form dimers in the anionic form, leads invariably to 1:1 stoichiometries. Finally, a study of the conductivity and magnetic properties of the CT complexes has demonstrated how subtle and unpredictable structural changes influence the physical characteristics of such materials.

Experimental Section

General experimental techniques have been described earlier.[3]

[Fe(η^5-$C_5Me_4SMe)_2]_3$(TCNQ)$_7$ (4). Fe(η^5-$C_5Me_4SMe)_2$ (**1**)[60] (100 mg; 0.256 mmol) and TCNQ (121 mg; 0.597 mmol) were dissolved in a minimal amount of acetonitrile, filtered, and cooled to −20 °C. The product crystallized as black thin platelets. Yield: 116 mg (52%). Mp: 185 °C (dec). Anal. Calcd for $C_{144}H_{118}N_{28}S_6Fe_3$: C, 66.51; H, 4.57; N, 15.08. Found: C, 66.53; H, 4.69; N, 15.32. IR (KBr): 2163, 1562, 1523, 1420, 1322, 1125, 953, 834, 700, 597. Single crystals for an X-ray analysis were obtained by dissolving the product in a minimal amount of acetonitrile followed by slow evaporation of the solvent at room temperature.

[Fe(η^5-$C_5Me_4S^tBu)_2$](TCNQ)$_3$ (5) was obtained as described for **4** from 40 mg (0.084 mmol) of Fe(η^5-$C_5Me_4S^tBu)_2$ (**2**)[60] and 69 mg (0.32 mmol) of TCNQ. Yield: 76 mg (83%) as black crystals. Mp: 195−200 °C (dec). Anal. Calcd for $C_{62}H_{54}N_{12}S_2Fe$: C, 68.50; H, 5.01; N, 1546. Found: C, 68.65; H, 4.96; N, 15.47. IR (KBr): 2168, 1566,1331, 1136, 695. Single crystals for an X-ray analysis have been obtained by dissolving the product in a minimal amount of acetonitrile and slow evaporation of the solvent at room temperature.

[Fe(η^5-$C_5Me_4S)_2S$](TCNQ)$_2$ (6) was obtained as described for **4** from 50 mg (0.13 mmol) of Fe(η^5-$C_5Me_4S)_2S$ (**3**),[60] 58 mg (0.28 mmol) of TCNQ, and 600 mg (NBu_4)(BF_4) in hot acetonitrile. The solvent was slowly evaporated over 1 week at 58 °C. Yield: 90 mg (89%) as black dendritic crystals. Mp: 200 °C (dec). Anal. Calcd for $C_{42}H_{32}N_8S_3Fe$: C, 62.99; H, 4.03; N, 13.99. Found: C, 63.04; H, 4.21; N, 13.80. IR (KBr): strong absorption above 1000 cm^{-1}, broad band at 700 cm^{-1}.

[Fe(η^5-$C_5Me_4SMe)_2$](TCNQF$_4$) (7) was obtained as described for **4** from 100 mg (0.27 mmol) of Fe(η^5-$C_5Me_4SMe)_2$ (**1**)[60] and 71 mg (0.27 mmol) of $TCNQF_4$.[62] Yield: 98 mg (57%) as black needles, suited for the X-ray analysis. Mp: 185−190 °C. Anal. Calcd for $C_{32}H_{30}N_4F_4S_2Fe$: C, 57.66; H, 4.54; N, 8.41. Found: C, 57.90; H, 4.51; N, 8.46. IR (KBr): 2928, 2849, 2194, 2175, 1635, 1536, 1497, 1695, 1337, 1264, 1196, 1141, 1026, 969, 870, 788, 717, 700, 564, 542, 464.

[Fe(η^5-$C_5Me_4S^tBu)_2$](TCNQF$_4$) (8) was obtained as described for **4** from 170 mg (0.36 mmol) of Fe(η^5-$C_5Me_4S^tBu)_2$ (**2**)[60] and 100 mg (0.36 mmol) of $TCNQF_4$. Yield: 127 mg (46%). Mp: 201 °C. Anal. Calcd for $C_{38}H_{42}N_4F_4S_2Fe$: C, 60.80; H, 5.64; N, 7.46. Found: C, 60.82; H 5.59; N, 7.60. IR (KBr): 2962, 2192, 2170, 1533, 1498, 1476, 1378, 1334, 1197, 1165, 1140, 1024, 965, 548.

[Fe(η^5-$C_5Me_4S)_2S$](TCNQF$_4$) (9) was obtained as described for **4** from 50 mg (0.13 mmol) of Fe(η^5-$C_5Me_4S)_2S$ (**3**)[60] and 35 mg (0.13 mmol) of $TCNQF_4$. Yield: 70 mg (81%) as black prisms which could be used directly for the X-ray analysis. Mp: >260 °C (dec). Anal. Calcd for $C_{30}H_{24}N_4F_4S_3Fe$: C, 53.89; H, 3.62; N, 8.38. Found: C, 53.85; H 3.61; N, 8.47. IR (KBr): 2923, 2195, 2177, 1632, 1535, 1496, 1395, 1338, 1264, 1196, 1142, 1021, 968, 870, 787, 714, 630, 560, 442, 524, 453.

[Fe(η^5-$C_5Me_5SMe)_2$](Br$_3$) (10). A 50 mg (0.128 mmol) sample of Fe(η^5-$C_5Me_5SMe)_2$ (**2**) was dissolved in a minimal amount of 1,2-dichloroethane, and 1 mL (0.23 mmol) of a bromine solution (0.23 M in 1,2-dichloroethane) was added. The green solution was filtered. Slow diffusion of *tert*-butylmethyl ether into this solution yielded **10** as black plates. Yield: 5.3 mg (7%). Mp: 161 °C. Anal. Calcd for $C_{20}H_{30}Br_3FeS_2$: C, 38.12; H, 4.80; S, 10.18. Found: C, 38.36; H, 481; S, 10.06. IR (KBr): 2912, 1422, 1376, 1309, 1020, 467.

[Fe(η^5-$C_5Me_5S^tBu)_2$](Br$_3$) (11) was obtained as described for **10** from 50 mg (0.105 mmol) of Fe(η^5-$C_5Me_5S^tBu)_2$ (**3**) in 1,2-dichloroethane and 0.83 mL (0.19 mmol) of a bromine solution (0.23 M in 1,2-dichloroethane). Yield: 35.8 mg (48%). Mp: 185 °C. Anal. Calcd for $C_{26}H_{42}Br_3FeS_2$: C, 43.72; H, 5.93; S, 8.98. Found: C, 43.84; H, 5.88; S, 9.03. IR (KBr): 2979, 2958, 2918, 2891, 1473, 1454, 1376, 1362, 1222, 1165, 1025, 574, 533, 491, 452.

[Fe(η^5-$C_5Me_5S)_2S$](Br$_3$) (12) was obtained as described for **10** from 50 mg (0.127 mmol) of Fe(η^5-$C_5Me_5S)_2S$ (**4**) in 1,2-dichloroethane and 0.83 mL (0.19 mmol) of a bromine solution (0.23 M in 1,2-dichloroethane). Yield: 64.4 mg (80%). Mp: 161 °C. Anal. Calcd for $C_{18}H_{24}Br_3FeS_3$: C, 34.20; H, 3.83; S, 15.22. Found: C, 34.21; H, 3.77; S, 15.12. IR (KBr): 2912, 1494, 1379, 1148, 1016, 522.

[Fe(η^5-$C_5Me_5SMe)_2$](I$_3$) (13) was obtained as described for **10** from 100 mg (0.256 mmol) of Fe(η^5-$C_5Me_5SMe)_2$ (**2**) and 97 mg (0.768 mmol) of iodine in 5 mL of 1,2-dichloroethane. Yield: 142 mg (72%). Mp: 170 °C. Anal. Calcd for $C_{20}H_{30}I_3FeS_2$: C, 31.15; H, 3.92; S, 8.32. Found: C, 31.40; H, 3.86; S, 8.55. IR (KBr): 2950, 2911, 1438, 1374, 1311, 1019, 976, 668, 570.

[Fe(η^5-$C_5Me_5S^tBu)_2$](I$_3$) (14) was obtained as described for **10** from 100 mg (0.21 mmol) of Fe(η^5-$C_5Me_5S^tBu)_2$ (**3**) and 80 mg (0.63 mmol) of iodine. Yield: 160 mg (88%). Mp: 221 °C. Anal. Calcd for $C_{26}H_{42}I_3FeS_2$: C, 36.51; H, 4.95; S, 7.50. Found: C, 36.50; H, 4.76; S, 7.53. IR (KBr): 2963, 2923, 2899, 2863,1474, 1452, 1377, 1363, 1223, 1166, 1026, 574, 533, 491, 452.

[Fe(η^5-$C_5Me_5S)_2S$](I$_3$) (15) was obtained as described for **10** from 100 mg (0.25 mmol) of Fe(η^5-$C_5Me_5S)_2S$ (**4**) and 97 mg (0.765 mmol) of iodine. Yield: 190 mg (96%). Mp: 222 °C. Anal. Calcd for $C_{18}H_{24}I_3FeS_3$: C, 27.96; H, 3.13; S, 12.44. Found: C, 27.94; H, 2.99; S, 12.18. IR (KBr): 2909, 1472, 1439, 1376, 1022, 623, 526, 456, 400, 370, 334.

X-ray Crystallographic Study of 4, 5, 7, 9, 11, 12, 14, and 15. Crystals suited for an X-ray analysis were obtained by slow evaporation of the solvent at room temperature or slow cooling to −20 °C of a hot saturated solution for the TCNQ- and $TCNQF_4$-containing compounds (**4**, **5**, **7**, and **9**) and by slow diffusion of *tert*-butylmethyl ether into a saturated solution, in the case of the trihalogenide salts (**11**, **12**, **14,** and

(62) Martin, E. L.; Wheland, R. C. *J. Org. Chem.* **1975**, *40*, 3101−3109.

15). Selected crystallographic and relevant data collection parameters are listed in Tables 1 and 2. Data were measured at room temperature (293(2) K) with variable scan speed to ensure constant statistical precision on the collected intensities. One standard reflection was measured every 120 reflections, and no significant variation was detected. The structures were solved by direct or Patterson methods and refined by full-matrix least-squares using anisotropic displacement parameters for all non-hydrogen atoms. The contribution of the hydrogen atoms in their idealized position (riding model with fixed isotropic $U = 0.080$ Å^2) was taken into account but not refined. All calculations were carried out by using the Siemens SHELX93 (VMS) system.

Conductivity Measurements. Samples of the CT complexes (ca. 80−100 mg) were pressed into pellets, and temperature-dependent conductivity was measured by the standard two-probe method.

Magnetic Measurements. The magnetic susceptibility χ of the charge-transfer complexes **4**−**15** was measured in the temperature range 2−300 K in an external variable magnetic field, by means of a Quantum Design superconducting quantum interference device (SQUID) magnetometer. The polycrystalline samples were mounted in a sample holder tube made of quartz glass in order to keep the magnetic background as low as possible. Routine corrections for core diamagnetism, temperature-independent paramagnetism, and the sample holder were applied.

Acknowledgment. S.Z. is grateful to the Swiss National Science Foundation for financial support (Grant 20-41974.94).

Supporting Information Available: Tables of atomic coordinates, complete listing of bond distances and angles, tables of anisotropic displacement coefficients, and coordinates of hydrogen atoms, as well as ORTEP representations and atom-numbering schemes for **4**, **5**, **7**, **9**, **11**, **12**, **14**, and **15**. This material is available free of charge via the Internet at http://pubs.acs.org. Tables of calculated and observed structure factors may be obtained from the authors upon request.

OM9902075